Bulgarian Chemical Communications, Volume 51, Issue 4 (pp. 513 - 520) 2019 DOI: 10.34049/bcc.51.4.4987

Modelling the interaction and prediction of mictrotubule assembly inhibition of podophyllotoxin and its derivatives by molecular docking

M. D. Atanasova[1*], P. Sasheva[2], I. M. Yonkova[2], I. A. Doytchinova[1]

[1]*Department of Chemistry, Faculty of Pharmacy, Medical University – Sofia, Bulgaria*
[2]*Department of Pharmacognosy, Faculty of Pharmacy, Medical University – Sofia, Bulgaria*

Received October 17, 2018; Accepted June 1, 2019

The interactions of 15 podophyllotoxin derivatives (synthetic and naturally occurring) within the colchicine binding site of β-tubulin were modelled by molecular docking. The docking protocol was optimized in terms of scoring function, radius of binding site and number of flexible amino acids within the binding site. Each docking run was repeated tree times and the average fitness score was correlated with the pID_{50}. The *Pearson*'s correlation coefficient *r* was 0.655. The derived model was validated by cross-validation in 5 groups. The differences between pID_{50exp} and pID_{50pred} of the studied compounds were less than one log unit for 93% of the compounds. The inhibitory activities of three new natural compounds were predicted. One of them, 4'-demethyl-6-methoxypodophyllotoxin, showed predicted ID_{50} value of 0.36 μM, placing this compound as one of most active inhibitors. This is in agreement with its known cytotoxicity which is 2 to 3.5 times higher than the cytotoxicity of etoposide in the different cell lines. The tubulin inhibition was suggested as a probable mechanism of the cytotoxicity of this compound.

Keywords: podophyllotoxin, molecular docking, modelling, colchicine binding site, microtubule inhibition, quantitative relationships

INTRODUCTION

Microtubules (MTs) are hollow, cylindrical organelles that play critical roles in diverse cellular processes. One of their essential functions is the participation in cell division as the main structure units of mitotic spindle, thus being responsible for the arranged segregation of replicated chromosomes into daughter cells [1, 2]. MTs of cytoskeleton together with actin filaments and intermediate filaments play a major role in determining and retaining the dynamic spatial organization of cytoplasm, as well as in specifying the characteristic cell shape [3]. Additionally, microtubules are the main structural components of eucariotic cilia and flagella [4]. They are involved in the elongated neuronal processes and in the intracellular transport [5,6].

As the microtubules are essential for the cell growth and division, they are target for a wide variety of substances, which mostly bind the protein tubulin [7-9]. Tubulin, the building block of microtubules, is a 100 kDa heterodimer formed by α- and β-polypeptides, that are equivalent in size and structure [10, 11]. Each tubulin subunit is a product of multiple genes, called isotypes [12]. Additional posttranslational modifications can be accomplished to both subunits, as polyglutamylation, polyglycylation, reversible tyrosination, phosphorylation and acetylation [12, 13]. Apart from the acetylation of Lys40, the main site for posttranslational modifications is the specific for each isotype C-terminal region, which is highly acidic and unstructured and is lying as a flexible arm at the MT lattice surface [11, 13]. Nevertheless, the major tubulin isotypes are highly conserved and typically containing only 2-8 % amino acid sequence divergence [14]. There are many specific binding sites on a tubulin heterodimer. The β-tubulin is much more known, as it is the main target of multiple ligands that hinder microtubule dynamics, several of which are anticancer drugs [15, 16]. The suppression of microtubule dynamics is a casual link in mitosis [17] and is realized by microtubule detachment (vinblastine, colchicine) or by hyperstabilisation of mictrotubule organizing centres (paclitaxel) [12]. Usually, the inhibitors bind to one of the three distinct sites – the colchicine, vinblastine and taxol sites [18, 19]. Despite the high degree of conservation between the isoforms, the geometry of the ligand binding site is specific for each of the β-tubulin isotypes, possibly rendering differences in binding affinities [20]. Interestingly, the majority of differences between the isoforms are found outside the ligand binding sites and concentrated in lateral and longitudinal surfaces, changing the overall kinetics of microtubule assembly and disassembly [21, 22].

Podophyllotoxin (Fig. 1) is a naturally occurring lignan [23] that destabilises the microtubules, causing arrest in the cell division [24]. The molecule competes for a colchicine-binding site of a soluble tubulin dimer.

* To whom all correspondence should be sent:
E-mail: matanasova@ddg-pharmfac.net

The presence of ligand in the tubulin dimer disturbs the interaction between the helices of α- and β-tubulin, which are involved in adopting straight conformation. Failure to lock straight conformation results in loss of lateral contact thus preventing microtubule assembly [19, 25]. Podophyllotoxin, like most of the microtubule-binding agents is needed only in small concentrations to inhibit the microtubule growth [26]. There are several characteristics of the podophyllotoxin interaction with the β-tubulin: podophyllotoxin binds to β-tubulin faster than the colchicine, does not activate GTP hydrolysis, and does not interact with the α-subunit T5 loop [25, 27]. These properties make podophyllotoxin a potential chemotherapeutic agent and trials for anticancer activity were done in humans [28, 29]. Although the adverse effects, as high gastrointestinal toxicity, have restricted its application as antineoplastic agent [30, 31], it is widely used for the local treatment of genital warts [32]. The remarkable biological activity makes podophyllotoxin an important source for developing of less toxic analogues. Thus the semi-synthetic anticancer drugs etoposide, teniposide and etopophos were developed. Despite of the structural similarity to podophyllotoxin, they act as topoisomerase II inhibitors [32-35]. Nowadays they are used for the treatment of Hodgkin's disease, small cell anaplastic lung cancer, testicular cancer and other malignancies [33, 36, 37]. The success of podophyllotoxin-based drugs made podophyllotoxin skeleton an attractive lead in the synthesis and isolation of novel active analogues [38].

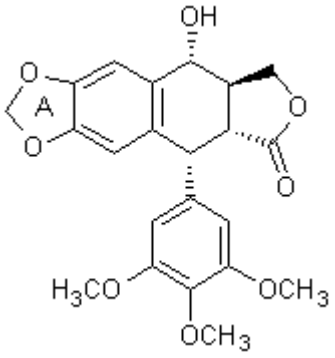

Figure 1. Structure of podophyllotoxin

In the present study, we applied molecular docking to model the binding of podophyllotoxin derivatives (synthetic and naturally occurring) within the colchicine binding site of β-tubulin in order to derive a quantitative relationship between the docking-based scores of the complexes and the microtubule inhibition. The derived relationship was validated by cross-validation in 5 groups. The lowest-energy pose of the most active microtubule inhibitor in the study was used to analyse the interactions between β-tubulin and inhibitor. The derived relationship was used to predict the activities of novel podophyllotoxin derivatives.

MATERIALS AND METHODS

Homology modelling

In the present study, the inhibition of microtubule assembly by podophylotoxin and its congeners was conducted on chicken brain tubulin [39]. As X-ray data for chicken tubulins are absent, the X-ray structure of cattle brain tubulin-podophyllotoxin complex (pdb code 1SA1) [19] was used as a template for homology modelling of the binding site. The binding site consists of 38 residues identified within a distance of 8Å from podophyllotoxin in the colchicine-binding site (Fig. 2).

There are seven isotypes of chicken β-tubulin, as isotypes β-II and β-III are dominant in brain [40, 41]. They were compared with the X-ray structure of cattle tubulin by sequence alignment (Figure 2). The binding site is highly conserved and only single mutations are available at positions 200, 239, 316, 330 and 351. The chicken isoforms IIa (given as P09203 TBB1_CHICK in Figure 2) and IIb (given as P32882 TBB2_CHICK in Figure 2) have one single mutation V316I. The substitution of Val with the bulkier Ile narrows the binding site [14]. Single point mutation of the X-ray bovine β-tubulin was performed to generate the V316I isoform, followed by MM optimization with AMBER03 force field. No water molecules are present in the binding site. The V316I isoform was used as a target in the subsequent docking simulations.

Data set and microtubule inhibition

The structures of the studied compounds and their inhibition on the microtubule assembly are given in Scheme 1. Compounds **1-8**, **15** and **1t-3t** have natural origin [39, 42], while compounds **9-14** are synthetic congeners of podophyllotoxin.

The inhibitory activity is measured as ID_{50} and it ranges from 0.2 μM to 30 μM.

```
1SA1:B|PDBID|CHAIN|SEQUENCE mreivhiqagqcgnqigakfwevisdehgidptgsyhgdsdlqlerinvyyneaagnkyv 60
SP|P09203|TBB1_CHICK        mreivhiqagqcgnqigakfwevisdehgidptgsyhgdsdlqlerinvyyneaagnkyv 60
SP|P32882|TBB2_CHICK        mreivhiqagqcgnqigakfwevisdehgidptgsyhgdsdlqlerinvyyneatgnkyv 60
SP|P09206|TBB3_CHICK        mreivhlqagqcgnqigakfwevisdehgidptgtyhgdsdlqlerinvyyneatggkyv 60
SP|P09652|TBB4_CHICK        mreivhiqagqcgnqigakfwevisdehgidpsgnyvgdsdlqlerisvyyneasshkyv 60
SP|P09653|TBB5_CHICK        mreivhiqagqcgnqigtkfwevisdehgidpaggyvgdsalqlerinvyynesssqkyv 60
SP|P09207|TBB6_CHICK        mreivhlqigqcgnqigakfwevisdehgidiagnycgnaslqlerinvyfneayshkyv 60
SP|P09244|TBB7_CHICK        mreivhiqagqcgnqigakfwevisdehgidptgtyhgdsdlqldrisvyyneatggkyv 60

1SA1:B|PDBID|CHAIN|SEQUENCE prailvdlepgtmdsvrsgpfgqifrpdnfvfgqsgagnnwakghytegaelvdsvldvv 120
SP|P09203|TBB1_CHICK        prailvdlepgtmdsvrsgpfgqifrpdnfvfgqsgagnnwakghytegaelvdsvldvv 120
SP|P32882|TBB2_CHICK        prailvdlepgtmdsvrsgpfgqifrpdnfvfgqsgagnnwakghytegaelvdsvldvv 120
SP|P09206|TBB3_CHICK        pravlvdlepgtmdsvrsgpfrqifrpdnfvfgqsgagnnwakghytegaelvdsvldvv 120
SP|P09652|TBB4_CHICK        prailvdlepgtmdsvrsgafghlfrpdnfifgqsgagnnwakghytegaelvdsvldvv 120
SP|P09653|TBB5_CHICK        pravlvdlepgtmdsvrsgpfgqlfrpdnfifgqtgagnnwakghytegaelvdsvldvv 120
SP|P09207|TBB6_CHICK        prsilvdlepgtmdsvrsskigplfrpdnfihgnsgagnnwakghytegaelienvmdvv 120
SP|P09244|TBB7_CHICK        prailvdlepgtmdsvrsgpfgqifrpdnfvfgqsgagnnwakghytegaelvdsvldvv 120

1SA1:B|PDBID|CHAIN|SEQUENCE rkesescdclqgfqlthslgggtgsgmgtlliskireeypdrimntfsvvpspkvsdtvv 180
SP|P09203|TBB1_CHICK        rkesescdclqgfqlthslgggtgsgmgtlliskireeypdrimntfsvmpspkvsdtvv 180
SP|P32882|TBB2_CHICK        rkesescdclqgfqlthslgggtgsgmgtlliskireeypdrimntfsvmpspkvsdtvv 180
SP|P09206|TBB3_CHICK        rkeaescdclqgfqlthslgggtgsgmgtlliskireeypdrimntfsvvpspkvsdtvv 180
SP|P09652|TBB4_CHICK        rkecencdclqgfqlthslgggtgsgmgtlliskvreeypdrimntfsvvpspkvsdtvv 180
SP|P09653|TBB5_CHICK        rkecehcdclqgfqlthslgggtgsgmgtlliskireeypdrimntfsvmpspkvsdtvv 180
SP|P09207|TBB6_CHICK        rnecescdclqgfqlihslgggtgsgmgtllinkireeypdrimntfsvvpspkvsdtvv 180
SP|P09244|TBB7_CHICK        rkeaescdclqgfqlthslgggtgsgmgtlliskireeypdrimntfsvvpspkvsdtvv 180

1SA1:B|PDBID|CHAIN|SEQUENCE epynatlsvhqlventdEtYcidnealydicfrtlklttptygdlnhlvsatmsgvTTCL 240
SP|P09203|TBB1_CHICK        epynatvsvhqlventdEtYcidnealydicfrtlklttptygdlnhlvsatmsgvTTCL 240
SP|P32882|TBB2_CHICK        epynatlsvhqlventdEtYcidnealydicfrtlklttptygdlnhlvsatmsgvTTCL 240
SP|P09206|TBB3_CHICK        epynatlsvhqlventdEtYcidnealydicfrtlklttptygdlnhlvsatmsgvTTCL 240
SP|P09652|TBB4_CHICK        epynatlsihqlventdEtYcidnealydicfrtlklatptygdlnhlvsatmsgvTTSL 240
SP|P09653|TBB5_CHICK        epynatlsvhqlventdEtYcidnealydicfrtlklttptygdlnhlvsatmsgvTTSL 240
SP|P09207|TBB6_CHICK        epynailsihqlientdEtFcidnealydicfrtlkltnptygdlnhlvsltmsgvTTSL 240
SP|P09244|TBB7_CHICK        epynatlsvhqlventdEtYcidnealydicfrtlklttptygdlnhlvsatmsgvTTCL 240

1SA1:B|PDBID|CHAIN|SEQUENCE RFpgQLNaDLRKLaVNMVpfprlhfFmpgfapltsrgsqqyraltvpeltqqmfdaknmm 300
SP|P09203|TBB1_CHICK        RFpgQLNaDLRKLaVNMVpfprlhfFmpgfapltsrgsqqyraltvpeltqqmfdsknmm 300
SP|P32882|TBB2_CHICK        RFpgQLNaDLRKLaVNMVpfprlhfFmpgfapltsrgsqqyraltvpeltqqmfdsknmm 300
SP|P09206|TBB3_CHICK        RFpgQLNaDLRKLaVNMVpfprlhfFmpgfapltsrgsqqyraltvpdltqqmfdaknmm 300
SP|P09652|TBB4_CHICK        RFpgQLNaDLRKLaVNMVpfprlhfFmpgfapltrrgsqqyraltvpeltqqmfdaknmm 300
SP|P09653|TBB5_CHICK        RFpgQLNaDLRKLaVNMVpfprlhfFmpgfapltargsqqyraltvpeltqqmfdaknmm 300
SP|P09207|TBB6_CHICK        RFpgQLNaDLRKLaVNMVpfprlhfFmpgfapltargsqqyralsvpeltqqmfdarnmm 300
SP|P09244|TBB7_CHICK        RFpgQLNaDLRKLaVNMVpfprlhfFmpgfapltsrgsqqyraltvpeltqqvfdaknmm 300

1SA1:B|PDBID|CHAIN|SEQUENCE aacdprhgryLTVaaVFrgrmsmkevdeqMlnvqnknssyfvewIpNNVKTaVCdipprg 360
SP|P09203|TBB1_CHICK        aacdprhgryLTVaaIFrgrmsmkevdeqMlnvqnknssyfvewIpNNVKTaVCdipprg 360
SP|P32882|TBB2_CHICK        aacdprhgryLTVaaIFrgrmsmkevdeqMlnvqnknssyfvewIpNNVKTaVCdipprg 360
SP|P09206|TBB3_CHICK        aacepghgryLTVaaVFrgrmsmkevdeqMlnvqnknssyfvewIpNNVKTaVCdipprg 360
SP|P09652|TBB4_CHICK        aacdprhgryLTVatVFrgrmsmkevdeqMlaiqsknssyfvewIpNNVKVaVCdipprg 360
SP|P09653|TBB5_CHICK        aacdprhgryLTVatVFrgpmsmkevdeqMlaiqnknssyfvewIpNNVKVaVCdipprg 360
SP|P09207|TBB6_CHICK        aacdprrgryLTVacIFrgrmstrevdeqLlsvqtknssyfvewIpNNVKVaVCdipprg 360
SP|P09244|TBB7_CHICK        aacdprhgryLTVaaVFrgrmsmkevdeqMlnvqnknssyfvewIpNNVKTaVCdipprg 360

1SA1:B|PDBID|CHAIN|SEQUENCE lkmsaTfIgNstaiqelfkriseqftamfrrkaflhwytgegmdemefteaesnmndlvs 420
SP|P09203|TBB1_CHICK        lkmsaTfIgNstaiqelfkriseqftamfrrkaflhwytgegmdemefteaesnmndlvs 420
SP|P32882|TBB2_CHICK        lkmsaTfIgNstaiqelfkriseqftamfrrkaflhwytgegmdemefteaesnmndlvs 420
SP|P09206|TBB3_CHICK        lkmsaTfIgNstaiqelfkriseqftamfrrkaflhwytgegmdemefteaesnmndlvs 420
SP|P09652|TBB4_CHICK        lkmssTfIgNstaiqelfkriseqftamfrrkaflhwytgegmdemefteaesnmndlvs 420
SP|P09653|TBB5_CHICK        lkmasTfIgNstaiqelfkriseqfsamfrrkaflhwftgegmdemefteaesnmndlvs 420
SP|P09207|TBB6_CHICK        lkmaaTfIgNntaiqelfirvseqfsamfrrkaflhwytgegmdemefseaegntndlvs 420
SP|P09244|TBB7_CHICK        lkmavTfIgNstaiqelfkriseqftamfrrkaflhwytgegmdemefteaesnmndlvs 420

1SA1:B|PDBID|CHAIN|SEQUENCE eyqqyqdatadeqgefeeegeedea---- 445
SP|P09203|TBB1_CHICK        eyqqyqdatadeqgefeeegeedea---- 445
SP|P32882|TBB2_CHICK        eyqqyqdatadeqgefeeegeedea---- 445
SP|P09206|TBB3_CHICK        eyqqyqdataeeegefeeeaeeeae---- 445
SP|P09652|TBB4_CHICK        eyqqyqdataeeegemyeddeeeseqgak 449
SP|P09653|TBB5_CHICK        eyqqyqeatandgeeafeddeeeine--- 446
SP|P09207|TBB6_CHICK        eyqqyqdatadveeyeeaeaspeket--- 446
SP|P09244|TBB7_CHICK        eyqqyqdataeeeedfgeeaeeea----- 444
```

Figure 2. Sequence alignment of the X-ray structure of cattle brain tubulin and the seven isotypes of chicken β-tubulin. The residues of the colchicine-binding site are given by capital letters.

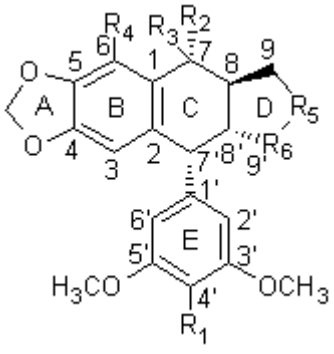

Common structure

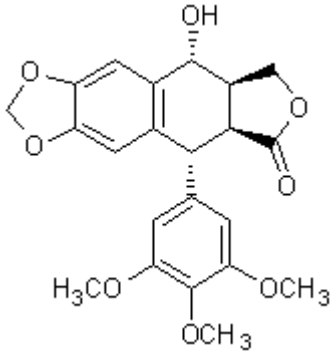

Picropodophyllotoxin
15

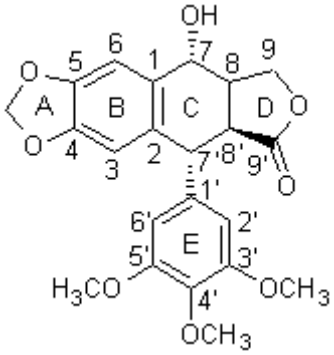

5'-Demethyl-6-methoxypodophyllotoxin
2t

No	Compound	R_1	R_2	R_3	R_4	R_5	R_6	ID_{50}(μM)
1	Podophyllotoxin	OCH_3	OH	H	H	O	C=O	0.6
2	Epipodophyllotoxin	OCH_3	H	OH	H	O	C=O	5
3	Deoxypodophyllotoxin	OCH_3	H	H	H	O	C=O	0.5
4	β-Peltatin	OCH_3	H	H	OH	O	C=O	0.7
5	4'-Demethylpodophyllotoxin	OH	OH	H	H	O	C=O	0.5
6	4'-Demethylepipodophyllotoxin	OH	H	OH	H	O	C=O	2
7	4'-Demethyldeoxypodophyllotoxin	OH	H	H	H	O	C=O	0.2
8	α-Peltatin	OH	H	H	OH	O	C=O	0.5
9	Podophyllotoxin-cyclic ether	OCH_3	OH	H	H	O	CH_2	1
10	Deoxypodophyllotoxin-cyclic ether	OCH_3	H	H	H	O	CH_2	0.8
11	Deoxypodophyllotoxin-cyclopentane	OCH_3	H	H	H	H_2	CH_2	5
12	Deoxypodophyllotoxin-cyclopentanone	OCH_3	H	H	H	C=O	CH_2	5
13	Podophyllotoxin-cyclic sulfide	OCH_3	OH	H	H	S	CH_2	10
14	Deoxypodophyllotoxin-cyclic sulfide	OCH_3	H	H	H	S	CH_2	10
15	Picropodophyllotoxin							30
1t	4'-Demethyl-6-methoxypodophyllotoxin	OH	OH	H	OCH_3	O	C=O	
2t	5'-Demethyl-6-methoxypodophyllotoxin							
3t	6-Methoxypodophyllotoxin	OCH_3	OH	H	OCH_3	O	C=O	

Scheme 1. Structures and inhibition of microtubule assembly of podophyllotoxin and its derivatives. Compounds **1** – **15** compose the training set; compounds **1t** – **3t** are newly isolated compounds [42], not tested.

The effects of different concentrations of podophyllotoxin and its derivatives on microtubule assembly were determined spectrophotometrically at 350 nm on a Gilford spectrophotometer equipped with an automatic recorder and Haake RK2 thermostatically regulated liquid circulator to maintain constant temperature [39]. The changes in turbidity occurred when unassembled tubulin in the presence of GTP in MES buffer at 37° *in vitro* polymerizes to form microtubules. The absorption of each drug at 350 nm was initially measured. There are no changes in turbidity when inhibition of microtubule assembly occurs.

Docking Protocol

The docking simulations in the present study were performed by GOLD v.5.2.2 software [43]. The protocol was optimized in terms of scoring

function, radius of the binding site and flexible residue side chains within the binding site in order to correlate best with pID_{50} ($-logID_{50}$). Four scoring functions, available in GOLD (ChemPLP, GoldScore, ChemScore and ASP), were compared at the following settings: flexible ligands, fixed protein and radius of the binding site 6Å. Four radiuses of the binding site were tested: 5Å, 6Å, 7Å and 8Å at fixed protein and flexible ligands. Up to 10 flexible residues in the binding site were selected stepwise in order to improve the correlation score/pID_{50}. Each run included 10 poses. The poses were ranked by two criteria: 1) rmsd (root mean square deviation) lower than 1.5Å and 2) highest fitness score. Only the highest-scored pose with rmsd < 1.5Å was considered. Each docking run was repeated three times and the average fitness score was used for correlation with the pID_{50}. The correlation was evaluated by the *Pearson*'s correlation coefficient *r* and evaluated by *leave-group-out cross-validation* coefficient q^2.

RESULTS AND DISCUSSION

Optimization of the Docking Protocol

The molecular docking procedure was optimized stepwise in terms of scoring function, radius and side-chain flexibility of the binding site.

Selection of scoring functions. GOLD v.5.2.2 [43] provides four scoring functions (SFs): ChemPLP, ChemScore, GoldScore and ASP. They were applied on the training set at the following settings: rigid protein, flexible ligand and radius of the binding site 6Å (Table 1). GoldScore had the highest correlation coefficient *r* with the pID_{50} (0.467) and it was selected as a SF used further in the study.

Radius of the binding site. The radius of the binding site was changed from 5Å to 8Å. The docking simulations were run with GoldScore, fixed protein and flexible ligands. The best correlation between docking score and inhibition of microtubule assembly was at 7Å (r = 0.509).

Table 1. Optimization of the docking protocol. Selected settings are given in bold.

Steps	*r*	Settings
1. Selection of SF		Rigid protein, flexible ligand, radius of the binding site 6Å
ChemScore	0.224	
ChemPLP	-0.114	
GoldScore	**0.467**	
APS	0.210	
2. Radius of the binding site		Gold Score, rigid protein, flexible ligand
5Å	0.392	
6Å	0.476	
7Å	**0.509**	
8Å	0.470	
3. Flexibility of the binding site		Gold Score, flexible ligand, radius of the binding site 7Å
200Tyr	0.532	
236Val	0.576	
240Leu	**0.597**	
241Arg	0.555	
247Asn	**0.599**	
250Leu	**0.602**	
255Val	0.514	
313Val	0.521	
317Phe	0.512	
347Asn	0.570	
349Val	0.583	
247Asn and 200Tyr	0.643	
247Asn and 256Asn	0.643	
250Leu and 237Thr	**0.655**	

Flexibility of the binding site. Each residue within the radius of 7Å was set flexible and the effect was rendered by the GoldScore/pIC_{50} correlation coefficient. The residues 240Leu, 247Asn and 250Leu showed the highest correlations. A second flexible residue was added to each of them and all combinations were screened. The best combinations are given in Table 1. The addition of a third flexible residue does not increase the correlation.

The optimized docking protocol includes the following settings: GoldScore, flexible ligand, radius of the binding site 7Å and two flexible residues (250Leu and 237Thr).

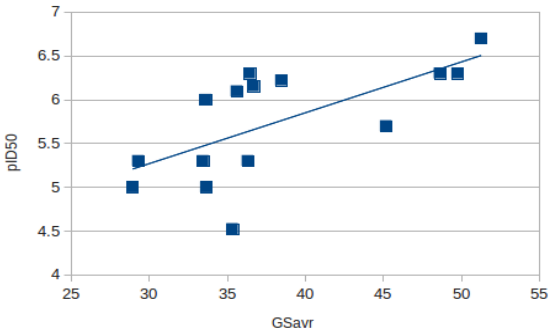

Figure 3. Linear relationship between pID_{50} and GoldScore.

Linear Relationship between GoldScore and pID_{50}.

Between pID_{50} and the GoldScore values derived by the optimized docking protocol exists a moderate linear relationship (Fig. 3) given by the following equation:

$$pID_{50} = 0.0581*GoldScore + 3.5297$$
$$n = 15,\ r = 0.655$$

The relationship was validated by leave-group-out cross-validation and the derived q^2 was 0.371. The differences between the experimental and predicted pID_{50} values were below 1 log unit, with the exception of picropodophyllotoxin (Table 2).

The microtubule inhibition of the three newly isolated compounds (**1t** – **3t**) was predicted by the derived relationship (Table 3). The activities of 5'-demethyl-6-methoxypodophyllotoxin (**2t**) and 6-podophyllotoxin (**3t**) are expected to be moderate with ID_{50} values of 3.79 and 4.47, respectively. However, the inhibitory activity of 4'-demethyl-6-methoxypodophyllotoxin (**1t**) is very high with predicted ID_{50} value of 0.36 μM placing the compound among the most active microtubule inhibitors. This prediction is in a good agreement with the high cytotoxicity of **1t** which is 2 to 3.5 times higher than that of etoposide in different human leukemic cell lines [44]. The present study suggests that the probable mechanism of action of 4'-demethyl-6-methoxypodophyllotoxin is inhibition of microtubule assembly.

Table 2. Experimental and predicted by cross-validation pID_{50} values.

No	Compound	pID_{50} exp.	pID_{50} pred.	$pID_{50\ exp}$ - pID_{50} pred.
1	Podophyllotoxin	6.22	5.83	0.39
2	Epipodophyllotoxin	5.30	5.63	-0.33
3	Deoxypodophyllotoxin	6.30	5.64	0.66
4	β-Peltatin	6.15	5.60	0.55
5	4'-Demethylpodophyllotoxin	6.30	6.46	-0.16
6	4'-Demethylepipodophyllotoxin	5.70	6.18	-0.48
7	4'-Demethyldeoxypodophyllotoxin	6.70	6.40	0.29
8	α-Peltatin	6.30	6.37	-0.07
9	Podophyllotoxin-cyclic ether	6.00	5.48	0.52
10	Deoxypodophyllotoxin-cyclic ether	6.10	5.59	0.51
11	Deoxypodophyllotoxin-cyclopentane	5.30	5.57	-0.27
12	Deoxypodophyllotoxin-cyclopentanone	5.30	5.19	0.11
13	Podophyllotoxin-cyclic sulfide	5.00	5.17	-0.17
14	Deoxypodophyllotoxin-cyclic sulfide	5.00	5.48	-0.48
15	Picropodophyllotoxin	4.52	5.67	-1.15

Table 3. Predicted ID_{50} values for the newly isolated podophyllotoxin derivatives.

No	Compound	ID_{50pred} (μM)
1t	4'-Demethyl-6-methoxypodophyllotoxin	0.36
2t	5'-Demethyl-6-methoxypodophyllotoxin	3.79
3t	6-Methoxypodophyllotoxin	4.47

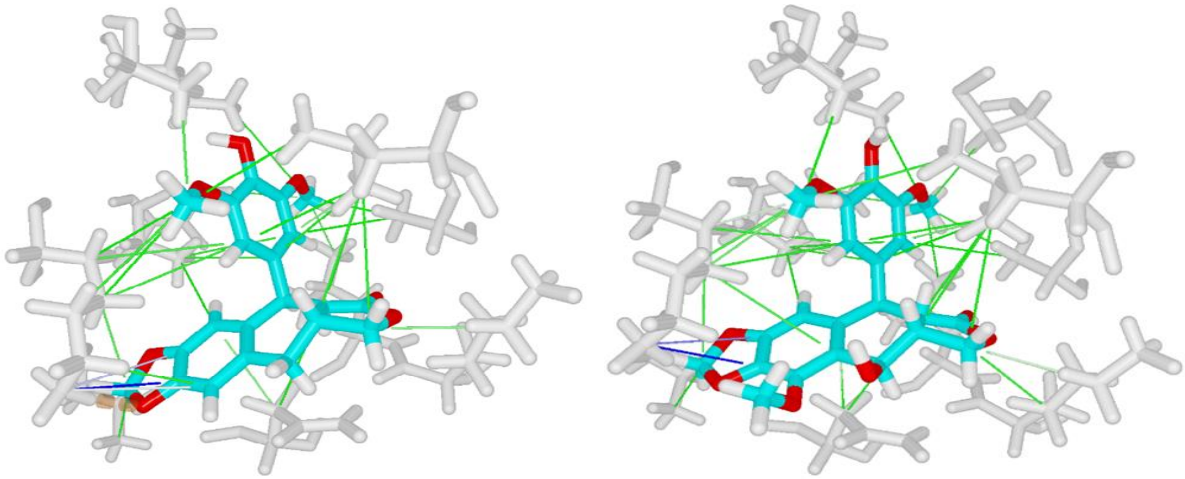

a) **b)**

Figure 4. Interactions between **a)** the most active compound **7** and tubulin, and **b)** the test compound **1t** and tubulin. Cation – π interaction is shown in blue, hydrophobic interactions – in green, and hydrogen bond – in dashed orange.

Interactions between Inhibitors and Tubulin

The interactions between the inhibitor 7 and tubulin within the colchicine binding site are given in Fig. 4a. Cation-π interaction exists between 350Lys and ring A from the ligand. A hydrogen bond is detected between 350Lys and O-atom in ring A. Many hydrophobic interactions occur between 4'-demethyldeoxypodophyllotoxin (compound 7) and the residues from the binding site. Very similar are the interactions between the newly isolated derivative 1t and tubulin (Fig. 4b).

CONCLUSION

In the present study the interaction of podophyllotoxin derivatives and colchicine binding site in chicken βII-tubulin isotypes IIa and IIb was modelled by molecular docking. The docking protocol was optimized in terms of scoring function, binding site radius and flexible residues within the binding site in order to correlate with the inhibitory activity of the compounds. The linear relationship between pID_{50} and GoldScore was validated by cross-validation in 5 groups. It was used to predict the inhibition of three newly isolated derivatives of podophylotoxin. One of them, 4'-demethyl-6-methoxy-podophyllotoxin, was predicted to be among the most active inhibitors of tubulin. Tubulin inhibition is a probable mechanism of the observed cytotoxicity of this compound.

REFERENCES

1. S. Inoue, *J. Cell Biol.*, **91**, 131 (1981).
2. J. D. Pickett-Heaps, D. H. Tippit, K. R. Porter, *Cell*, **29**, 729 (1982).
4. J. E. Heuser, M. W. Kirschner, *J. Cell Biol.*, **86 (1)**, 212 (1980).
5. I. R. Gibbons, in: Molecules and cell movement, S. Inoue, R. E. Stephens (eds.), Raven Press, New York, 1975, p. 207.
6. J. H. Hayden, R. D. Allen, *J. Cell Biol.*, ***99***, 1785 (1984).
7. R. D. Vale, B. J. Schnapp, T. S. Reese, M. Sheetz, *Cell*, **40**, 449 (1985).
8. L. C. Morejohn, D. E. Fosket, *Pharmacol. Ther.*, **51**, 217 (1991).
9. P. Kohler, *Int. J. Parasitol.*, **31**, 336 (2001).
10. A. Jordan, J. A. Hadfield, N. J. Lawrence, A. T. McGown, *Med. Res. Rev.*, **18**, 259 (1998).
11. R. F. Luduena, E. M. Shooter, L. Wilson, *J. Biol. Chem.*, **252**, 7006 (1977).
12. E. Nogales, *Annu. Rev. Biophys. Biomol. Struct.*, **30**, 397 (2001).
13. R. F. Ludueña, in: International Review of Cytology - a Survey of Cell Biology, K. W. Jeon, (ed.), vol. 178, Academic Press, San Diego, 1998, p. 207.
14. P. Verdier-Pinard, E. Pasquier, H. Xiao, B. Burd, C. Villard, D. Lafitte, L. M. Miller, R. H. Angeletti, S. B. Horwitz, D. Braguer, *Anal. Biochem.*, **384**, 197 (2009).

15. S. Sharma, B. Poliks, C. Chiauzzi, R. Ravindra, A. R. Blanden, S. Bane, *Biochem.*, **49 (13)**, 2932 (2010).
16. J. Huzil, R. F. Ludueña, J. Tuszynski, *Nanotechnology*, **17**, S90 (2006).
17. M. A. Jordan, L. Wilson, *Curr. Opin. Cell. Biol.*, **10**, 123 (1998).
18. T. Mitchison, M. Kirschner, *Nature*, **312**, 237 (1984).
19. M. Jordan, L. Wilson, *Nat. Rev. Canc.*, **4**, 253 (2004).
20. R. B. G. Ravelli, B. Gigant, P. A. Curmi, I. Jourdain, S. Lachkar, A. Sobel, M. Knossow, *Nature*, **428**, 198 (2004).
21. J. Huzil, P. Winter, L. Johnson, A. Weis, T. Bakos, A. Banerjee, R. F. Ludueña, S. Damaraju, J. Tuszynski, *Chem. Biol. Drug Des.*, **75**, 541 (2010).
22. J. T. Huzil, K. Chen, L. Kurgan, J. A. Tuszinsky, *Cancer Inform.*, **3**, 159 (2007).
23. C. A. Burkhart, M. Kavallaris, B. S. Horwitz, *Biochim. Biophys. Acta*, **1471**, O1 (2001).
24. I. Ionkova, *Pharmacog. Rev*., **1 (1)**, 57 (2007).
25. A. L. Parker, M. Kavallaris, J. A. McCarroll, *Front. Oncol.*, **4**, 153 (2014).
26. A. Dorleans, B. Gigant, R. B. G. Ravelli, P. Mailliet, V. Mikol, M. Knossow, *Proc. Natl. Acad. Sci.*, **106 (33)**, 13775 (2009).
27. R. A. Stanton, K. M. Gernet, J. H. Nettles, R. Aneja, *Med. Res. Rev.*, **31 (3)**, 443 (2011).
28. C. Wang, A. Cormier, B. Gigant, M. Knossow, *Biochem.*, **46**, 10595 (2007).
29. J. L. Hartwell, A. W. Shrecker, *Fortschr. Chem. Org. Naturstoffe*, **15**, 106 (1958).
30. M. G. Kelly, J. L. Hartwell, *J. Nat. Cancer Inst.*, **14**, 967 (1954).
31. H. Savel, *Proc. Am. Assoc. Cancer Res.*, **5**, 56 (1964).
32. H. Savel, *Progr. Exptl. Tumor Rae*., **8**, 189 (1966).
33. A. Koulman, W. J. Quax, N. Pras, in: Biotechnology of medicinal plants: vitalizer and therapeutic, K. G. Ramawat (ed.), Science Publishers Inc., Enfield (USA), Plymouth (UK), 2004, p. 225.
34. K. R. Hande, *Eur. J. Cancer*, **34**, 1514 (1998).
35. W. Ross, T. Rowe, B. Glisson, J. Yalowich, L. Liu, *Cancer Res.*, **44**, 5857 (1984).
36. A. J. Wozniak, W. E. Ross, *Cancer Res.*, **43**, 120 (1983).
37. H. L. McLeod, W. E. Evans, in: Cancer Medicine 4th Edition, J. F. Holland, R. C. Bast, D. L. Morton, E. III Frei, D. W. Kufe, R. R. Weichselbaum, (eds.), Williams & Wilkins: Baltimore, 1997, p. 259.
38. H. J. Wichers, G. G. Versluis-De Haan, J. W. Marsman, M. P. Harkes, *Phytochemistry*, **11**, 3601 (1991).
39. H. Saito, Y. Nishimura, S. Kondo, T. Takeuchi, H. Umezawa, *Bull. Chem. Soc. Jpn.*, **61**, 1259 (1988).
40. J. D. Loike, C. F. Brewer, H. Sternlicht, W. J. Gensler, S. B. Horwitz, *Cancer Res.*, **38**, 2688 (1978).
41. J. C. Havercroft, D. W. Cleveland, *J. Cell Biol.***, *99***, 1927 (1984).
42. R. F. Ludueña, *Mol. Biol. of the Cell*, **4**, 445 (1993).
43. P. Sasheva, I. Ionkova, N. Stoilova, *Nat. Prod. Commun.*, **10 (7)**, 1225 (2015).
44. G. Jones, P. Willett, R. C. Glen, A. R. Leach, R. Taylor, *J. Mol. Biol.*, **267**, 727 (1997).
45. N. Vasilev, G. Momekov, M. Zaharieva, S. Konstantinov, P. Bremner, M. Heinrich, I. Ionkova, *Neoplasma*, **52 (5)**, 425 (2005).